TIGER: Text-Instructed 3D Gaussian Retrieval and Coherent Editing

Teng Xu   Jiamin Chen   Peng Chen   Youjia Zhang   Junqing Yu   Wei Yang[†]
Huazhong University of Science and Technology
{tengxu, jiaminchen, pengchen, youjiazhang, yjqing, weiyangcs}@hust.edu.cn

Abstract

Editing objects within a scene is a critical functionality required across a broad spectrum of applications in computer vision and graphics. As 3D Gaussian Splatting (3DGS) emerges as a frontier in scene representation, the effective modification of 3D Gaussian scenes has become increasingly vital. This process entails accurately retrieve the target objects and subsequently performing modifications based on instructions. Though available in pieces, existing techniques mainly embed sparse semantics into Gaussians for retrieval, and rely on an iterative dataset update paradigm for editing, leading to over-smoothing or inconsistency issues. To this end, this paper proposes a systematic approach, namely TIGER, for coherent text-instructed 3D Gaussian retrieval and editing. In contrast to the top-down language grounding approach for 3D Gaussians, we adopt a bottom-up language aggregation strategy to generate a denser language embedded 3D Gaussians that supports open-vocabulary retrieval. To overcome the over-smoothing and inconsistency issues in editing, we propose a Coherent Score Distillation (CSD) that aggregates a 2D image editing diffusion model and a multi-view diffusion model for score distillation, producing multi-view consistent editing with much finer details. In various experiments, we demonstrate that our TIGER is able to accomplish more consistent and realistic edits than prior work. Result videos can be found on the project website: https://xutanxing.github.io/TIGER/.

1 Introduction

Object editing within three-dimensional scenes constitutes a critical functionality in digital modeling, with broad applications spanning movie/game development, architecture, virtual reality and etc. This editing process entails retrieve the objects to be edited and subsequently performing modifications based on instructions. Recent advancements in neural scene representations have expedited the digitization of real-world 3D scenes from multi-view images [1, 2, 3, 4], highlighting the necessity for retrieval and editing techniques that are compatible with these advancements. Pioneering researches have focused on developing editing methods tailored to implicit 3D scene representations [5, 6, 7, 8, 9, 10], particularly the Neural Radiance Field (NeRF) [11, 12, 13, 14, 15, 16]. Notably, the Instruct-NeRF2NeRF [17] introduces iterative dataset updating approach that leveraging an pre-trained image editing diffusion model [18] for text-driven NeRF scene editing. However, the implicit nature of NeRF poses significant challenges when instructed to edit a specific target object within the scene.

As 3D Gaussian Splatting (3DGS) [19] emerges as the new frontier in scene representation, the effective modification of 3D Gaussian scenes has attracted significant attention. Unlike implicit methods, 3DGS adopts 3D Gaussians as explicit geometric primitives, providing foundations for retrieval and editing operations. Recent endeavors, such as GaussianEditor-NTU [20] and GaussianEditor-HW [21], have adopted analogous methodologies for editing 3D Gaussian scenes. These methods

---

[†]Corresponding Author

Text Prompt: *"Turn the vase into copper, turn the white flower into cherry blossom, turn the lily into red rose."*

Figure 1: Our TIGER presents a systematic framework for 3D Gausssian retrieval and editing. TIGER integrates language features into each Gaussian primitive, and support open-vocabulary query directly in space. TIGER demonstrates excellent zero-shot retrieval capabilities, and enable detail preserving and multi-view consistent editing.

identify the target objects from 2D segmentation of images, then unproject the segmentation masks into space to determine the relevant 3D Gaussians for editing. Subsequently, they use an iterative dataset updating scheme, akin to Instruct-NeRF2NeRF, to optimize the targeted Gaussians based on evolving image inputs. Despite the notable achievements of these approaches, their reliance on image-guided retrieval necessitates repeated 2D segmentation for each editing operation, relies on optimal rendering perspectives for precise segmentation of the target, and the dataset updating scheme is prone to inducing over-smoothing and the multi-face Janus problem [17].

To tackle the aforementioned challenges, this paper introduces a systematic approach termed TIGER (**T**ext-**I**nstructed **G**aussian **R**etrieval and **E**diting). TIGER offers direct Gaussian retrieval in 3D space according to textual input, obviating the need for 2D image bridging, and introduces a detail-preserving, multi-view consistent editing paradigm. Specifically, to enable the retrieval of 3D Gaussians directly from textual prompts, we incorporate language embedding into each 3D Gaussian via differentiable rendering. Previous approaches for Gaussian grounding typically rely on 2D supervision from semantics [20, 21] or extract language feature within each distinct mask [22, 23]. However, such top-down strategies (segment and extract feature within a mask) constrain the diversity of queryable objects as language features are extracted within mask, and hence ignoring context outside mask. In response, we devise a bottom-up scheme utilizing MaskCLIP [24] to extract nuanced, low-level language features and subsequently employ FeatUp [25] to refine these features into a high-resolution language feature map for 3D Gaussian supervision. Our scheme provides open-vocabulary query directly in 3D space. For retrieval, we measure the relevancy score between each 3D Gaussian's language embedding and the object text query. Furthermore, for the editing process, we propose a novel Coherent Score Distillation Sampling (CSD) technique that integrates the SDS losses from both an image editing diffusion model and a multi-view diffusion model. We update the 3D Gaussians according to the CSD loss, applying a higher update rate to the more relevant Gaussians, and a lower rate conversely. This technique ensures that edits not only adhere to the textual prompt through the image editing diffusion model but also maintain consistency across multiple views via the multi-view diffusion model. In our implementation, we employ the pre-trained InstructPix2Pix [18] as the image editing diffusion model, which is adept at following detailed text directives for image transformations. We utilize MVDream [26] as the multi-view diffusion model to guarantee that the edits remain coherent when observed from different perspectives. This integrated approach facilitates a robust editing framework that upholds both fidelity to textual instructions and spatial consistency. Extensive experiments demonstrate that our TIGER supports accurate open-vocabulary retrieval, and is able to accomplish more consistent and realistic edits than prior work.

2 Related Works

3D langugae fields. The interaction between language and 3D has long been a focal point for vision researchers in the realm of visual studies [27, 28, 29, 30, 31, 32, 33, 34, 35]. NeRFs [11], widely recognized for producing photorealistic new perspectives of a scene from calibrated photographs, have gained popularity and have seen numerous extensions. In the realm of 3D technology, significant advancements have been made in integrating language, revolutionizing our interaction

with digital environments. LERF [36] embeds CLIP [37] features into NeRF [11], enabling more intuitive natural language interaction and providing extensive scene analysis. 3D-OVS [38] leverages pre-trained foundational models in a weakly supervised manner to distill neural radiance fields, effectively elevating 2D features to view-consistent 3D segmentation. Recent work has also introduced 3D Gaussian representations [19] into the domain of 3D language localization and segmentation, achieving more precise localization. LangSplat [22] proposes using SAM [39] to learn hierarchical semantics, eliminating the need for DINO [40] feature regularization. Additionally, they trained a scene-specific language autoencoder to reduce memory requirements, though their features remain hierarchical, necessitating multiple queries across different levels. FMGS [23] integrates visual language embeddings from foundational models into 3D Gaussian representations. They scale up the embeddings of the smaller scales in the pre-computed CLIP feature pyramid bilinearly to the largest scale feature map and generate a composite feature map by averaging these embeddings. In previous work, images were cropped and fed into CLIP to obtain features for each patch. This is also the primary reason why they require hierarchical processing. We, however, employ MaskCLIP [24] to directly generate dense semantic features, and then use FeatUp [25] to upsample these features to the pixel level. Consequently, we only need to train a single-layer language field, while still maintaining access to global information.

3D editing. Editing neural radiance fields (NeRF [11]) has become a popular research direction recently. However, due to the implicit representation of NeRF, there is a lack of precise localization for the editing objects. As a result, most of the editing work focuses on the entire 3D scene [41, 16, 42, 12, 43, 44, 14]. Some studies have focused on object-centric editing problems. For example, Instruct-NeRF2NeRF [17] uses text to control 3D scene editing, allowing constraints on the editing object through text. However, it relies solely on InstructPix2Pix [18] to control the background, often resulting in global modifications. DreamEditor [15] represents scenes as mesh-based neural fields and accurately edits specified areas based on text prompts. However, the quality and speed of editing are constrained by the scene representation. Recent work has introduced 3D Gaussians [19] into the field of 3D editing [21, 20], whose explicit representation can accurately localize the editing areas. GaussianEditor-NTU [20] introduces Gaussian semantic tracing, achieving precise editing. However, it still relies on an iterative dataset update paradigm for editing, which leads to issues such as over-smoothing or inconsistency. We successfully apply Coherent Score Distillation to 3D Gaussian editing, producing results that better adhere to the editing instructions and exhibit richer details.

3 Method

In this section, we introduce our TIGER method that offers open-vocabulary 3D Gaussian retrieval and detail-preserving, multi-view consistent editing. Specifically, we incorporate language embedding into each 3D Gaussian with supervision from a bottom-up language feature extraction scheme (section 3.1). And we propose a novel Coherent Score Distillation Sampling (CSD) technique that integrates the SDS losses from both an image editing diffusion model and a multi-view diffusion model (section 3.2) for consistent and realistic editing.

3.1 Language Embedded 3D Gaussian for Open-vocabulary Retrieval

Grounding language embedding into 3D Gaussians entails adding a language feature into each Gaussian primitive and optimizing them through supervision from images.

3D Language Gaussians 3D Gaussian Splatting represents a scene as a volume of anisotropic Gaussians, where each Gaussian is characterized by its position $u \in \mathbb{R}^3$, covariance $\Sigma \in \mathbb{R}^7$, color $c \in \mathbb{R}^3$ and opacity $o \in \mathbb{R}$. We specifically add another element, the language embedding vector $\mathcal{L} \in \mathbb{R}^{64}$ into each Gaussian and form the primitive of our representation: $\mathcal{G} = \{u, \Sigma, c, o, \mathcal{L}\}$. Blend ordered Gaussians $\mathcal{G}_i, i = 1...N$ along a pixel ray r and denote $\alpha_i = o_i G(x_i)$ which represents the influence of the i-th Gaussian to the image pixel, we can render out the language feature f of the pixel via a blending process:

$$f = \sum_{i=1}^{N} (\mathcal{L}_i \alpha_i \prod_{j=1}^{i-1} (1 - \alpha_j)) \tag{1}$$

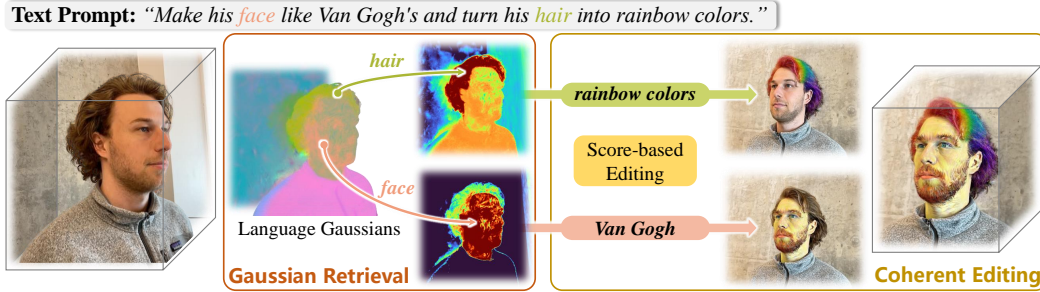**Text Prompt:** *"Make his face like Van Gogh's and turn his hair into rainbow colors."*

Figure 2: The pipeline of our method. We first embed language features into each Gaussian primitive. Upon receiving editing prompt, we compute a relevance score for each Gaussian w.r.t. the given edit prompt. Subsequently, we can update Gaussians using our CSD based on the relevancy scores.
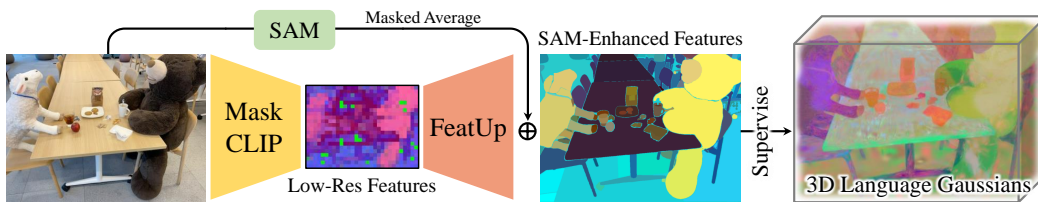

Figure 3: Our Language Embedding Process: we use MaskCLIP to generate low-resolution semantic features with global context information, then upsample the low-resolution features into high-resolution for 3D Gaussian language supervision using FeatUp [25]. To better preserve the sharp boundery, we apply SAM to the finest level and aggregate features with each fine mask. Finally, the refined language features are embedded into 3D Gaussians via differentiable rendering, enabling precise retrieval of relevant Gaussian points based on open-vocabulary query.

Bottom-up Language Feature Extraction To optimize the language embedding within each Gaussian, it is crucial to first transform the 2D image dataset into a per-pixel language feature map for effective supervision using Eqn. 1. The fidelity and granularity of this feature map are critical, as they directly influence the quality of the final language embedding. However, the language feature, i.e., CLIP [37], is extract from the whole image. Exiting endeavors, such as GaussianEditor-NTU [20], GaussianEditor-HW [21], rely on masks to tag each Gaussian, hence rely on 2D images for retrieving. LangSplat [22] and Gaussian Grouping [45], segment the images first and extract CLIP features [37] within each mask. However, these top-down strategies (segment and then extract language feature within each mash) constrains the capability for open-vocabulary queries. We propose an innovative bottom-up extraction method enabling precise and open-vocabulary retrieval of objects, laying a solid foundation for subsequent 3D editing tasks.

To generate the language feature map, we first use MaskCLIP to produce low-resolution patch-level language features. This patch feature encompass multi-scale global information through masked self-distillation features. This is fundamentally different from extracting features by cropping the image first and then inputting it into Clip. We then use FeatUp to upsample these features to pixel-level language features. To further save memory, we use PCA to the extracted CLIP feature dimension to 64 before supervision. During language embedding optimization, we only update $\mathcal{L}$ of each Gaussian while keeping all other properties unchanged.

Although the language feature is sufficient resolution for Gaussian supervision at this stage, they still suffer uneven bounderies.For further refinement, we apply SAM [39] at the finest level, and generate a set of fine binary masks M, we then conduct masked average to aggregate all the language features within each mask to obtain refined semantic boundaries. Notice our masked average process is fundamentally different to the top-down approach as our feature generated from MaskCLIP contains global information that across semantic boundaries. While extracting language features within each mask lead of the absence of context information outside the mask in the final language feature.

Open-vocabulary 3D Gaussian Retrieval   After optimization, we can directly retrieve 3D Gaussians using similarity between $\mathcal{L}$ and the textual object query $\mathcal{T}$. Thanks to the bottom-up feature extraction, our language embedding contains both local and global context information, hence support open-vocabulary querying. Given an arbitrary object query, our method achieves excellent zero-shot localization capability, as shown in Fig. 6. It's quite intuitive to directly retrieve an object $\mathcal{O}$ using a embedded text prompt $\mathcal{T}^*$ according to the cosine similarity with their language embedding $\mathcal{L}$.

$$\mathcal{O} = \{\mathcal{G} : \langle \mathcal{T}^* \cdot \mathcal{G}(\mathcal{L}) \rangle > \tau\} \tag{2}$$

where τ is the relevancy threshold. Notice our representation also supports image level query as we can render the language embedding into images according to Eq. 1, and calculate the relevancy score. Different from LERF and LanSplat, which require computing relevancy score across multiple scales and levels and taking the highest score, our method only needs to conduct one level of computation.

3.2   Coherent Score Distillation for Gaussian Editing

Building upon the language-embedded 3D Gaussians, we can perform scene editing instructed by the text prompts. Our method takes the reconstructed 3D Gaussian scene and language prompt $\mathcal{T}$ for editing as input. As output, our method generates an edited version of the Gaussian scene according to the provided instructions. Existing 3D Gaussian editing methods unanimously adopt the iterative dataset updating scheme [20, 21], which induces over-smoothing and multi-face Janus problem as the editing of each image is independent. To address the issue, we propose a novel Coherent Score Distillation (CSD) that integrate the SDS losses of a 2D image editing diffusion model, i.e., the InstructPix2Pix, and a multi-view diffusion model, i.e., the MVDream, producing multi-view consistent editing with fine details. An overview is provided in Fig. 4.

For a 3D Gaussian scene $\mathbf{S} = \{\mathcal{G}_i\}$, we retrieve 3D Gaussians according to the relevance scores w.r.t. the text prompt, and calculate the center and bounding box of the targeted object. Accordingly, we then choose four camera views $v_i, i = 1, 2, 3, 4$ around the targeted object (every $90°$ for $360°$ scenes, and evenly distributed between bounds for other scenarios) and render the corresponding views $\mathbf{x}_{v_i} = \mathcal{R}(\mathbf{S}, v_i)$, where $\mathcal{R}$ denotes the differentiable rendering function. We use ϵ_ϕ to denote the Instruct-Pix2Pix model, which take
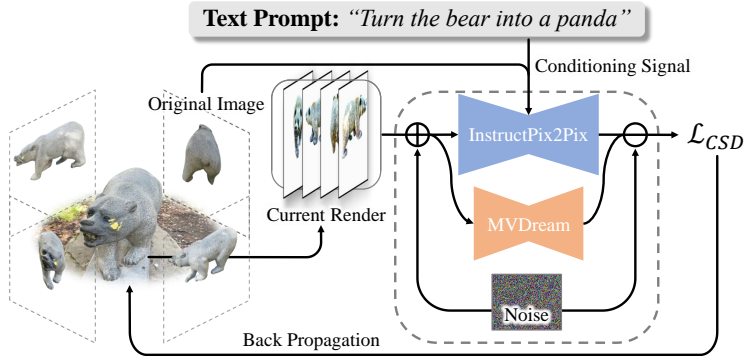

Figure 4: Our 2D Gaussian editing method use a Coherent Score Distillation that leverages 2D image editing diffusion model (Instruct-Pix2Pix) for instruct-based editing and utilizes multi-view diffusion model (MVDream) to address multi-face inconsistency issue, and achieve multi-view consistent edits with fine details.

a noisy image $\mathbf{x}_{v_i}^t = \mathbf{x}_{v_i} + \sigma_t\epsilon$ and edit text $\mathcal{T}$ as input and output the noise to be reduced. Similarly, we use ϵ_ψ to denote the MVDream model, which take noisy images from all four views $\{\mathbf{x}_{v_i}^t\}$, text $\mathcal{T}$ and camera view v_i as input and output the noise to be reduced of all four views. Consequently, the averaged noise residuals of ϵ_ϕ and ϵ_ψ on rendered views are as follows:

$$\mathcal{L}_{\mathbf{ip}} = \mathbb{E}_{t,\epsilon,i} \left[\omega(t) \left(\epsilon_\phi \left(\mathbf{x}_{v_i}^t; t, \mathbf{x}_{v_i}, \mathcal{T} \right) - \epsilon \right) \right], \mathcal{L}_{\mathbf{mv}} = \mathbb{E}_{t,\epsilon} \left[\omega(t) \left(\epsilon_\psi \left(\{\mathbf{x}_{v_i}^t\}; t, \{v_i\}, \mathcal{T} \right) - \epsilon \right) \right] \tag{3}$$

where $\omega(t)$ is a weighting function. Finally, we have our CSD as the combination of two SDS as:

$$\nabla_{\mathbf{S}} \mathcal{L}_{\mathbf{CSD}}(\mathbf{S}) = \mathbb{E}_{v_i} \left[(\lambda_1 \mathcal{L}_{\mathbf{ip}} + \lambda_2 \mathcal{L}_{\mathbf{mv}}) \frac{\partial \mathbf{x}_{v_i}}{\partial \mathbf{S}} \right] \tag{4}$$

λ_1 and λ_2 are weighting factors. For each iteration, we update the 3D Gaussians $\mathbf{S}$ using CSD loss, and then random a new set of four views, and add noises for the next round CSD loss calculation. In practice, we only add minor noise (t is chosen from 0.02 to 0.2) at each optimization step to ensure stable updates to the scene. And during score distillation, we always use the original 3D Gaussian

rendered views as conditions for InstructPix2Pix, thus effectively preventing unstable updates due to the excessive fluidity of 3D Gaussians as pointed out by GaussianEditor-NTU. Additionally, we employ a dynamic weighting strategy to blend the gradients of these two diffusion models, initially emphasizing the role of the multi-view diffusion model to prioritize generating consistent geometric structures. Later, we gradually increase the weight of the image editing diffusion model to sculpt details.

Score-based Updating   Each of our 3D Gaussian primitive is associated with a language embedding vector $\mathcal{L}$. With this language attribute, we compute its relevance score with respect to a textual query embedding $\mathcal{T}^*$ using cosine similarity, defined as $s_i = \langle \mathcal{T}^* \cdot \mathcal{G}_i(\mathcal{L}) \rangle$. To optimize the gradient of each Gaussian, we leverage the relevance score s_i to adjust the updating rate. This strategy enables higher update rates for more relevant Gaussians and smaller, or even zero, updates for less relevant ones, facilitating precise object-level editing. For 3D Gaussian updating and densification process, newly added Gaussians inherit the language vector $\mathcal{L}$ attribute of their parent Gaussians, and we selectively densify only the 3D Gaussians within the top 1% of gradient for each iteration to ensure more stable updates.

4   Experiments

In this section, we conduct extensive experiments to demonstrate the effectivenss of our TIGER.

4.1   Comparison with SOTA

Language Instructed Localization

To evaluate the open-vocabulary retrieval performance of our TIGER method, we compare with LERF and LangSplat which support open-vocabulary queries. We assess the 3D localization performance of our method using the LERF dataset [36]. The LERF dataset contains several large-scale scenes for object localization and retrieval. Following LERF, we use localization accuracy as the evaluation metric. We utilize the test views defined in LangSplat and employ text queries from both LERF and LangSplat for evaluation.

As shown in Tab. 1, our method achieves an overall accuracy of 87.0%, about 10 points higher than LangSplat and 15% better than LERF. Furthermore, our method achieves the highest localization accuracy in three out of four scenes, demonstrating its superiority in open-vocabulary retrieval abilities.

We also compare the retrieval performances qualitively and show the results in Fig. 5. We visualize the relevancy scores following LERF into a 2D map. Notice that, LERF and LangSplat necessity computation of the relevancy score across multiple semantic levels, while our method only requires one time computation and enables fine-grained localization at the same time. As illustrated in Fig. 6, the highest score positions of LangSplat are wrong

Test Scene	LERF	LangSplat	Ours
figurines	75.0%	75.5%	**83.7%**
teatime	84.8%	**91.5%**	84.8%
ramen	62.0%	67.7%	**91.9%**
waldo kitchen	72.7%	75.0%	**87.5%**
Overall	73.6%	77.4%	**87.0%**

Table 1: Localization accuracy comparison. Overall is calculated as the average across scenes.
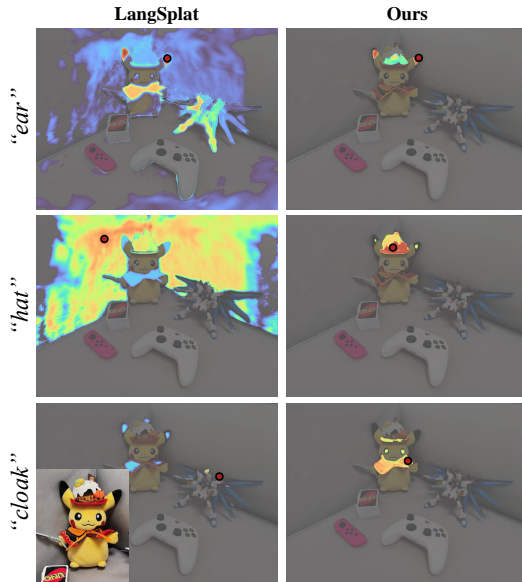

Figure 5: Qualitative comparison: TIGER method performs well in fine-grained localization.

for 'nori', 'wavy noodles' and the 'red cup', whereas our method accurately locates them. Though the location of the reported highest score is correct for LERF, the activated regions of LERF are very scattered. In contrast, our method produces very clear boundaries and more concentrated activation regions compared to those of LERF and LangSplat.
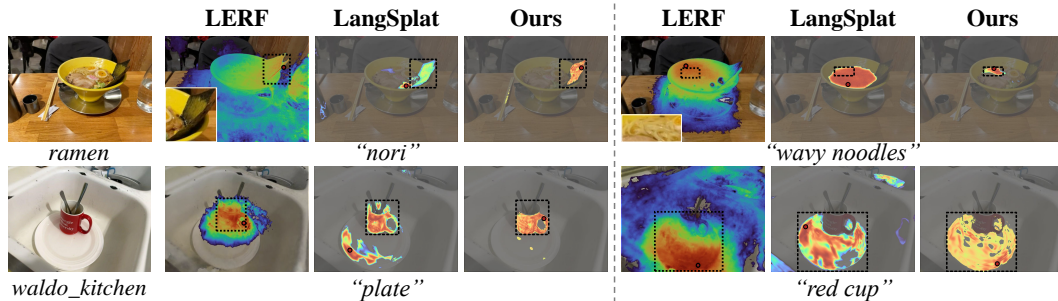

Figure 6: Comparison of the generated relevance score maps on the LERF dataset: the black bounding boxes are the ground truth and the red points are the localization results. Notice, the ground-truth of 'wavy noodles' is only a small corner area and our result is very accurate.
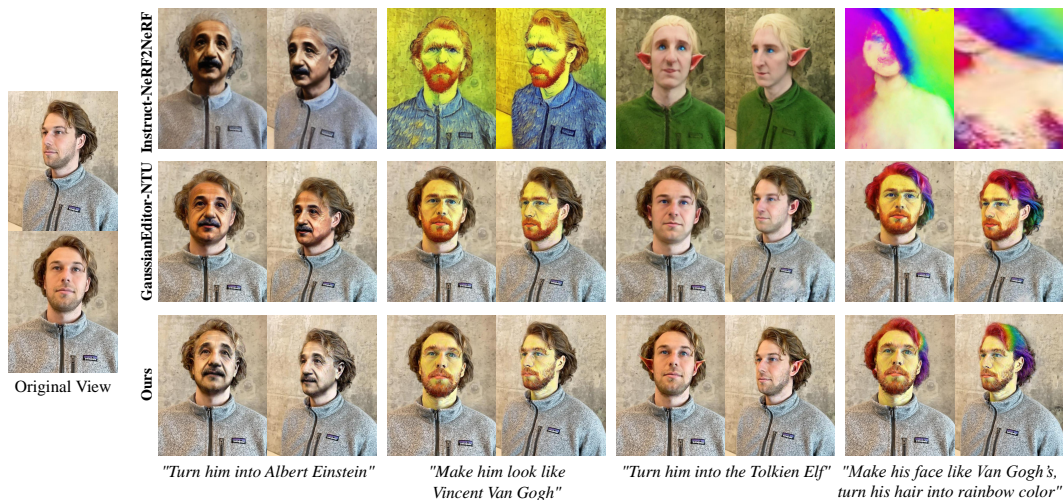

Figure 7: Qualitative comparison: Our method enables various types of portrait editing, including celebrities, artistic styles, characters from fantasy novels, and well support composite edits. Our edits exhibit very fine details, realistic and are view-consistent.

Figure 8: Qualitative comparison: Instruct-NeRF2NeRF is unable to perform partial edits, and GaussianEditor-HW produces blurry and inconsistent results. In contrast, our method generates precise and multi-view consistent human part edits.

3D Gaussian Editing We compare our 3D Gaussian editing performance with Instruct-NeRF2NeRF [17], GaussianEditor-NTU [20] and GaussianEditor-HW [21] on various datesets
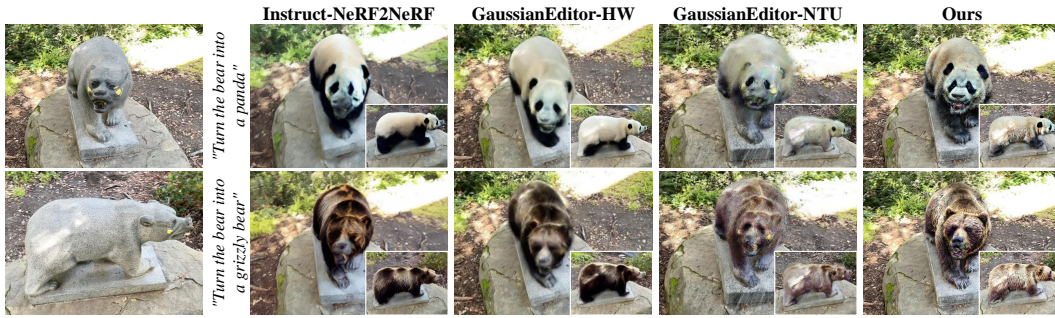
Figure 9: Qualitative comparison: our results of 'panda' and 'grizzly bear' show very fine fur and facial details. While other approaches suffer over-smoothing and the multi-face Janus problem.

"Make it Autumn"   "Make it snowy"

Figure 10: Qualitative results: environmental changes.

including the 'bear' and 'face' scene from Instruct-NeRF2NeRF. We implement our language embedding on LangSplat [22] and editing for 3D Gaussian on Threestudio [46]. All our experiments were conducted on a single Tesla V100S GPU. Depending on the prompt and the complexity of the scene, the editing process typically requires optimization for 1200 to 3000 steps, taking approximately 10 to 30 minutes in total. More experimental details will be provided in the appendix. The experiments results are shown in Fig. 9 and Fig. 7 repsectively. As we can see, for the bear scene in Fig. 9, our results contain much finer details and the bear heads of the edited results are consistent. In contrast, other approches suffer over-smoothing and Janus problems to different extent. Moreover, for the 'face' scene, our eidts are more consistent with the original video and more coherent. Instruct-NeRF2NeRF doens't support multi-round editing, while GaussianEditor-NTU generates blurry faces, and fails for the '*Tolkien Elf*' edits.

"Turn the sheep into a golden retriever, turn the bear into a raccoon"

"Turn the table into yellow color, turn the vase into a blue porcelain"

Figure 11: Compositional editing: Our approach enables multi-object compositional editing without mutual interference. The edits show very fine details. Notice the blurriness in background of the 'tea-time' scene is due to input blurry images in the dataset.

8

4.2 Qualitative Evaluation

To demonstrate that our TIGER can handle various scenes and prompts, we visualize more results of our TIGER on environment editing prompts and compositional editing prompts as shown in Fig. 10 and Fig. 11 respectively. As show in Fig. 10, our TIGER edits the 3D Gaussian scene in very subtle way, see the yellow leaves for 'autumn' and snow in 'snowy' edits. Moreover, we our method can handle large appearance edits as shown in Fig. 11. The results of 'dog' and 'raccoon' are very accurate and realistic, and the 'table' and 'vase' also show very subtle change, while preserving the textures of original object.

4.3 Ablations

To demonstrate our design choices, we conduct ablation studies on using MVDream for CSD, and our score-based 3D Guassian updating.

MVDream. We demonstrate effectiveness of MVDream in CSD by gradually increasing the MV-Dream loss weight and show result in Fig. 12. It can be seen that as the MVDream weight increases, the multi-face Janus issue gradually alleviated.

Relevance score based updating. To demonstrate the effect of score constraints on Gaussian updates, we demonstrate the results without the constraint of relevance score on the gradient in Fig. 13. As we can see that, the modifications tend to affect the entire scene, background wall turns yellowish, without score based updating constraints.
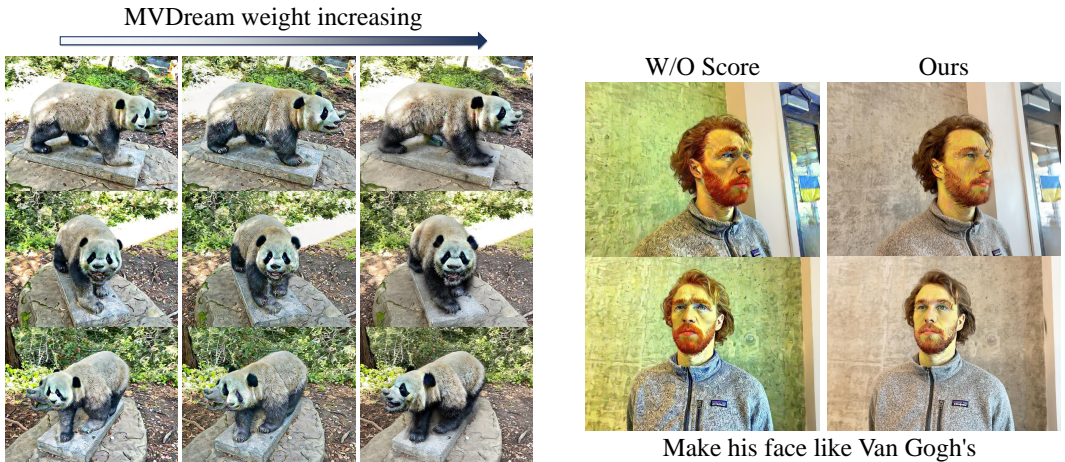

Figure 12: Ablation: MVDream alleviate the multi-face Janus issue.

Figure 13: Ablation: score-base updating limits the editing area.

5 Conclusion

This paper proposes a systematic approach, namely TIGER, for coherent text-instructed 3D Gaussian retrieval and editing.TIGER adopts a bottom-up language aggregation strategy to generate a denser language embedded 3D Gaussians that supports open-vocabulary retrieval. It also incorporates a Coherent Score Distillation (CSD) that aggregates a 2D image editing diffusion model and a multi-view diffusion model, producing multi-view consistent editings with much more fine details. In various experiments, our TIGER is able to accomplish more consistent and realistic edits than prior work.

Limitations. We adopt the MaskCLIP to extract language features, hence it also suffers the "bag-of-words" problem, where phrases like "not red" are treated similarly to "red". Our editing process depends on pre-trained 2D diffusion models, it is limited in handling highly complex instructions. Additionally, the score distillation process requires up-to 30 minutes for the most extensive edits. Although it's comparable to, and occasionally quicker than, GaussianEditor-NTU based on our testing, such prolonged processing times are still deemed excessively lengthy for practical user applications.

References

[1] Yu, A., R. Li, M. Tancik, et al. Plenoctrees for real-time rendering of neural radiance fields. In *Proceedings of the IEEE/CVF International Conference on Computer Vision*, pages 5752–5761. 2021.

[2] Fridovich-Keil, S., A. Yu, M. Tancik, et al. Plenoxels: Radiance fields without neural networks. In *Proceedings of the IEEE/CVF Conference on Computer Vision and Pattern Recognition*, pages 5501–5510. 2022.

[3] Müller, T., A. Evans, C. Schied, et al. Instant neural graphics primitives with a multiresolution hash encoding. *ACM transactions on graphics (TOG)*, 41(4):1–15, 2022.

[4] Chen, Z., T. Funkhouser, P. Hedman, et al. Mobilenerf: Exploiting the polygon rasterization pipeline for efficient neural field rendering on mobile architectures. In *Proceedings of the IEEE/CVF Conference on Computer Vision and Pattern Recognition*, pages 16569–16578. 2023.

[5] Park, J. J., P. Florence, J. Straub, et al. Deepsdf: Learning continuous signed distance functions for shape representation. In *Proceedings of the IEEE/CVF conference on computer vision and pattern recognition*, pages 165–174. 2019.

[6] Liu, S., Y. Zhang, S. Peng, et al. Dist: Rendering deep implicit signed distance function with differentiable sphere tracing. In *Proceedings of the IEEE/CVF Conference on Computer Vision and Pattern Recognition*, pages 2019–2028. 2020.

[7] Vicini, D., S. Speierer, W. Jakob. Differentiable signed distance function rendering. *ACM Transactions on Graphics (TOG)*, 41(4):1–18, 2022.

[8] Mescheder, L., M. Oechsle, M. Niemeyer, et al. Occupancy networks: Learning 3d reconstruction in function space. In *Proceedings of the IEEE/CVF conference on computer vision and pattern recognition*, pages 4460–4470. 2019.

[9] Chen, Z., H. Zhang. Learning implicit fields for generative shape modeling. In *Proceedings of the IEEE/CVF conference on computer vision and pattern recognition*, pages 5939–5948. 2019.

[10] Lombardi, S., T. Simon, J. Saragih, et al. Neural volumes: Learning dynamic renderable volumes from images. *arXiv preprint arXiv:1906.07751*, 2019.

[11] Mildenhall, B., P. P. Srinivasan, M. Tancik, et al. Nerf: Representing scenes as neural radiance fields for view synthesis. *Communications of the ACM*, 65(1):99–106, 2021.

[12] Wang, C., M. Chai, M. He, et al. Clip-nerf: Text-and-image driven manipulation of neural radiance fields. In *Proceedings of the IEEE/CVF Conference on Computer Vision and Pattern Recognition*, pages 3835–3844. 2022.

[13] Park, J., G. Kwon, J. C. Ye. Ed-nerf: Efficient text-guided editing of 3d scene with latent space nerf. In *The Twelfth International Conference on Learning Representations*. 2023.

[14] Wang, C., R. Jiang, M. Chai, et al. Nerf-art: Text-driven neural radiance fields stylization. *IEEE Transactions on Visualization and Computer Graphics*, 2023.

[15] Zhuang, J., C. Wang, L. Lin, et al. Dreameditor: Text-driven 3d scene editing with neural fields. In *SIGGRAPH Asia 2023 Conference Papers*, pages 1–10. 2023.

[16] Huang, Y.-H., Y. He, Y.-J. Yuan, et al. Stylizednerf: consistent 3d scene stylization as stylized nerf via 2d-3d mutual learning. In *Proceedings of the IEEE/CVF Conference on Computer Vision and Pattern Recognition*, pages 18342–18352. 2022.

[17] Haque, A., M. Tancik, A. A. Efros, et al. Instruct-nerf2nerf: Editing 3d scenes with instructions. In *Proceedings of the IEEE/CVF International Conference on Computer Vision*, pages 19740–19750. 2023.

[18] Brooks, T., A. Holynski, A. A. Efros. Instructpix2pix: Learning to follow image editing instructions. In *Proceedings of the IEEE/CVF Conference on Computer Vision and Pattern Recognition*, pages 18392–18402. 2023.

[19] Kerbl, B., G. Kopanas, T. Leimkühler, et al. 3d gaussian splatting for real-time radiance field rendering. *ACM Transactions on Graphics*, 42(4):1–14, 2023.

[20] Chen, Y., Z. Chen, C. Zhang, et al. Gaussianeditor: Swift and controllable 3d editing with gaussian splatting. *arXiv preprint arXiv:2311.14521*, 2023.

[21] Fang, J., J. Wang, X. Zhang, et al. Gaussianeditor: Editing 3d gaussians delicately with text instructions. *arXiv preprint arXiv:2311.16037*, 2023.

[22] Qin, M., W. Li, J. Zhou, et al. Langsplat: 3d language gaussian splatting. *arXiv preprint arXiv:2312.16084*, 2023.

[23] Zuo, X., P. Samangouei, Y. Zhou, et al. Fmgs: Foundation model embedded 3d gaussian splatting for holistic 3d scene understanding. *arXiv preprint arXiv:2401.01970*, 2024.

[24] Zhou, C., C. C. Loy, B. Dai. Extract free dense labels from clip. In *European Conference on Computer Vision*, pages 696–712. Springer, 2022.

[25] Fu, S., M. Hamilton, L. Brandt, et al. Featup: A model-agnostic framework for features at any resolution. *arXiv preprint arXiv:2403.10516*, 2024.

[26] Shi, Y., P. Wang, J. Ye, et al. Mvdream: Multi-view diffusion for 3d generation. *arXiv:2308.16512*, 2023.

[27] Zhi, S., T. Laidlow, S. Leutenegger, et al. In-place scene labelling and understanding with implicit scene representation. In *Proceedings of the IEEE/CVF International Conference on Computer Vision*, pages 15838–15847. 2021.

[28] Siddiqui, Y., L. Porzi, S. R. Buló, et al. Panoptic lifting for 3d scene understanding with neural fields. In *Proceedings of the IEEE/CVF Conference on Computer Vision and Pattern Recognition*, pages 9043–9052. 2023.

[29] Kobayashi, S., E. Matsumoto, V. Sitzmann. Decomposing nerf for editing via feature field distillation. *Advances in Neural Information Processing Systems*, 35:23311–23330, 2022.

[30] Tschernezki, V., I. Laina, D. Larlus, et al. Neural feature fusion fields: 3d distillation of self-supervised 2d image representations. In *2022 International Conference on 3D Vision (3DV)*, pages 443–453. IEEE, 2022.

[31] Gordon, D., A. Kembhavi, M. Rastegari, et al. Iqa: Visual question answering in interactive environments. In *Proceedings of the IEEE conference on computer vision and pattern recognition*, pages 4089–4098. 2018.

[32] Azuma, D., T. Miyanishi, S. Kurita, et al. Scanqa: 3d question answering for spatial scene understanding. In *proceedings of the IEEE/CVF conference on computer vision and pattern recognition*, pages 19129–19139. 2022.

[33] Cascante-Bonilla, P., H. Wu, L. Wang, et al. Simvqa: Exploring simulated environments for visual question answering. In *Proceedings of the IEEE/CVF Conference on Computer Vision and Pattern Recognition*, pages 5056–5066. 2022.

[34] Corona, R., S. Zhu, D. Klein, et al. Voxel-informed language grounding. *arXiv preprint arXiv:2205.09710*, 2022.

[35] Thomason, J., M. Shridhar, Y. Bisk, et al. Language grounding with 3d objects. In *Conference on Robot Learning*, pages 1691–1701. PMLR, 2022.

[36] Kerr, J., C. M. Kim, K. Goldberg, et al. Lerf: Language embedded radiance fields. In *Proceedings of the IEEE/CVF International Conference on Computer Vision*, pages 19729–19739. 2023.

[37] Radford, A., J. W. Kim, C. Hallacy, et al. Learning transferable visual models from natural language supervision. In *International conference on machine learning*, pages 8748–8763. PMLR, 2021.

[38] Liu, K., F. Zhan, J. Zhang, et al. Weakly supervised 3d open-vocabulary segmentation. *Advances in Neural Information Processing Systems*, 36:53433–53456, 2023.

[39] Kirillov, A., E. Mintun, N. Ravi, et al. Segment anything. In *Proceedings of the IEEE/CVF International Conference on Computer Vision*, pages 4015–4026. 2023.

[40] Caron, M., H. Touvron, I. Misra, et al. Emerging properties in self-supervised vision transformers. In *Proceedings of the IEEE/CVF international conference on computer vision*, pages 9650–9660. 2021.

[41] Huang, H.-P., H.-Y. Tseng, S. Saini, et al. Learning to stylize novel views. In *Proceedings of the IEEE/CVF International Conference on Computer Vision*, pages 13869–13878. 2021.

[42] Nguyen-Phuoc, T., F. Liu, L. Xiao. Snerf: stylized neural implicit representations for 3d scenes. *arXiv preprint arXiv:2207.02363*, 2022.

[43] Wu, Q., J. Tan, K. Xu. Palettenerf: Palette-based color editing for nerfs. *arXiv preprint arXiv:2212.12871*, 2022.

[44] Zhang, K., N. Kolkin, S. Bi, et al. Arf: Artistic radiance fields. In *European Conference on Computer Vision*, pages 717–733. Springer, 2022.

[45] Ye, M., M. Danelljan, F. Yu, et al. Gaussian grouping: Segment and edit anything in 3d scenes. *arXiv preprint arXiv:2312.00732*, 2023.

[46] Guo, Y.-C., Y.-T. Liu, R. Shao, et al. threestudio: A unified framework for 3d content generation. `https://github.com/threestudio-project/threestudio`, 2023.

A Appendix

A.1 Additional implementation details

In order to maintain consistency across multiple viewpoints, view dependent is cancelled. The Classifier-free guidance weights for InstructPix2Pix follow the default settings, with $S_I = 1.5$ and $S_T = 7.5$. For MVDream, the parameters from the official 3D generation repository are used, except for reducing max_step_percent to 0.2 to ensure update stability. The initial weight ratio of InstructPix2Pix to MVDream is set at $2:1$. Over time, the weight for InstructPix2Pix gradually increases while the weight for MVDream decreases until MVDream's weight reaches zero after 75% of the total training epochs. For scenes with environmental and minimal viewpoint changes, editing can rely entirely on InstructPix2Pix. FeatUp is implemented using the implicit upsampler from its official repository, with parameters following the default settings.

A.2 Delete objects

We eliminate the queried object from 3D Gaussians, render the remainings into training views, and identify holes from alpha map, which are inpainted using LaMa. We use inpainted images to retrain the 3D Gaussians. While texture consistency varies, this approach is effective for simple geometries, creating visually appealing results like the stone platform in Fig. 14.

"delete the bear"

Figure 14: Delete the bear.

A.3 More results

Turn the sheep into   *"a cow"*   *"a golden retriever"*   *Turn the bear into*   *"a raccoon"*   *"a tiger"*

Figure 15: More results of TIGER on the 'tea time' scene.

"Turn his pants into yellow"   *"Turn his pants into a bronze statue"*   *"Turn his t-shirt into sweater"*   *"Turn his t-shirt into green"*   *"Turn him into a bronze statue"*

Figure 16: More results of TIGER on partial body editing.
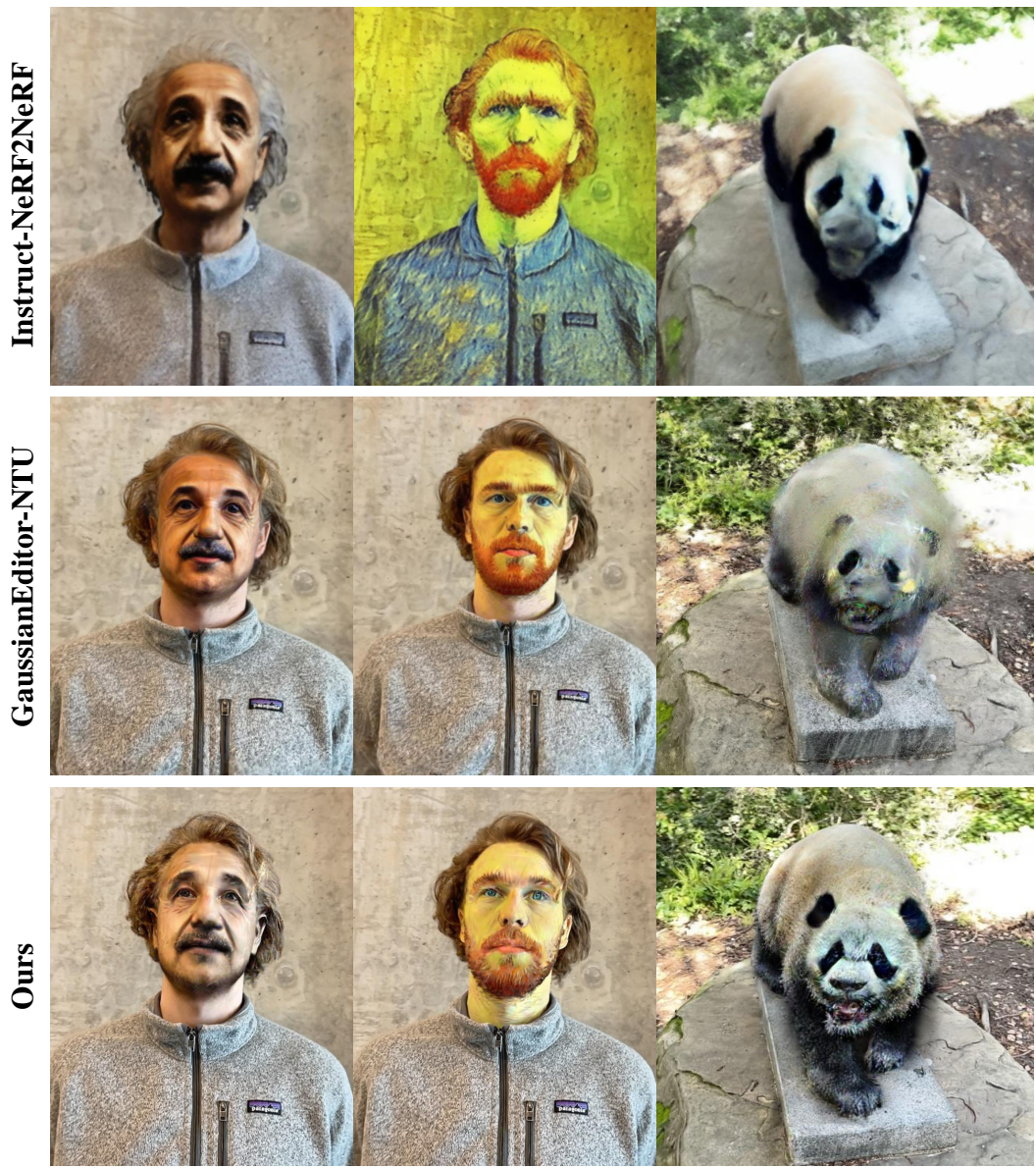
Figure 17: Details comparison.

| Original | *"Turn the lily into red rose"* | *"Turn the vase into copper"* |

Figure 18: Details.

| *"blue porcelain vase"* | *"green crystal vase"* | *"golden vase"* |
| *"yellow table"* | *"copper table"* | *"stone table"* |

Figure 19: More results of TIGER.